

How do slender mineral crystals resist buckling in biological materials?

BAOHUA JI, HUAJIAN GAO†

Max Planck Institute for Metals Research, Heisenbergstrasse 3,
D-70569, Stuttgart, Germany

and K. JIMMY HSIA

Department of Theoretical and Applied Mechanics,
University of Illinois, Urbana, IL 61801, USA

[Received in final form 15 July 2004 and accepted 22 October 2004]

ABSTRACT

Mineral crystals in biological materials such as bone, tooth, and sea shell are susceptible to buckling under compressive loading due to their slender geometry with large aspect ratios. How does nature deal with this problem? This question is especially interesting in view of the three orders of magnitude difference in elastic modulus between protein and mineral. As a first analysis of this question, we study the stability of a single mineral platelet confined in an otherwise perfect protein–mineral nanostructure. We find that there exists a transition of buckling strength from an aspect ratio-dependent regime to a lower threshold value, independent of the crystal geometry. Typical values of the aspect ratio of mineral crystals of bone and nacre fall in this transition region. The existence of a buckling strength independent of the detailed geometrical parameters of mineral may be critically important from the point of view of structure robustness as the composite behaviour of biomaterials should not depend sensitively on small variations in crystal size and shape.

§ 1. INTRODUCTION

Biological materials such as bone, tooth and sea shell have superior stiffness, strength, and toughness. These materials are organic–inorganic composites with complex hierarchical microstructures (Currey 1977, Jackson *et al.* 1988, Landis 1995, Rho *et al.* 1998, Weiner and Wagner 1998, Menig *et al.* 2000, Menig *et al.* 2001). Small angle X-ray scattering (SAXS), transmission electron microscopy (TEM), and high voltage electron microscopy (HVEM) have shown that the most elementary structure of many biological materials consists of mineral crystals with very large aspect ratios embedded in a soft protein matrix. Figure 1*a* illustrates that in bone and dentin the mineral platelets are 2–3 nm thick and up to 100 nm long (Landis 1995, Landis and Hodgens 1996, Fratzl *et al.* 1997, Tesch *et al.* 2001), and figure 1*b* shows that in nacre the platelets are 200–500 nm thick and 5–8 μm long (Kamat *et al.* 2000, Wang *et al.* 2001). Jäger and Fratzl (2000) and Gao *et al.* (2003) have developed simple mechanical models idealizing the nanostructure of these

†Email: hjgao@mf.mpg.de.

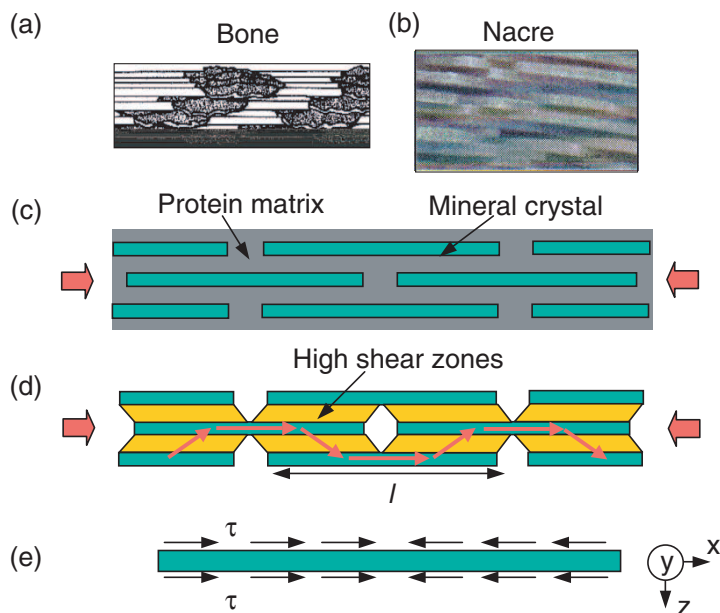


Figure 1. The generic nanostructure of bone-like biological materials. (a) bone; (b) nacre; (c) a schematic diagram of mineral crystals with large aspect ratios staggered in the protein matrix. (d) A tension-shear chain (TSC) model illustrating the primary force transfer route in the biological nanostructure; the mineral crystals carry most of the compressive load and protein transfers force between adjacent mineral crystals via shear. (e) The free-body diagram of a mineral crystal showing the compressive load due to shear stress applied along the sides of the crystal.

biological materials as staggered hard platelets aligned in a soft matrix (figure 1c). In this structure, the mineral platelets bear most of the tensile or compressive load while the protein matrix transfers forces between adjacent platelets via shear and also plays a number of other functions important for stress relaxation around the mineral crystals (Ji and Gao 2004a). The large aspect ratio of mineral platelets (as large as 30–40 in bone) is a critical feature enabling protein to transfer large forces at relatively small stress levels and the composite to have a stiffness close to its upper (Voigt) limit (Ji and Gao 2004b). Gao *et al.* (2003, 2004) and Gao and Ji (2003) proposed that the nanometre dimensions of the biomineral crystals may have been selected by natural evolution to achieve robustness against fracture in brittle solids: sufficiently small mineral crystals can maintain their theoretical strength despite of their brittleness and defects. The nanometre dimension and high strength of mineral crystals play a key role in the strength and fracture toughness of protein–mineral nanocomposites (Gao *et al.* 2004, Ji and Gao 2004b).

The hybrid organic–inorganic structure is one of the main characters of biological materials. The very large differences in mechanical properties of protein and mineral constituents allow biological materials to have unique and interesting behaviours in comparison with conventional composite materials. While mineral provides stiffness and hardness for the composite structure to carry mechanical loads, protein serves a multitude of support and relaxation functions including energy

absorption and dissipation, protecting mineral against fracture and impact, sensing damage, and initiating biological remodelling (Gao *et al.* 2004, Ji and Gao 2004a,b). An approximate formula for the stiffness of biocomposites can be derived from a simple tension-shear chain model described in figure 1 as (Gao *et al.* 2003)

$$\frac{1}{E} = \frac{4(1 - \Phi_M)}{G_P \Phi_M^2 \rho^2} + \frac{1}{\Phi_M E_M}, \tag{1}$$

where G_P is the shear modulus of protein; E_M , ρ , Φ_M are, respectively, the Young’s modulus, aspect ratio and volume concentration of mineral. Throughout the present paper, subscript “ M ” will be used to denote the properties of mineral and subscript “ P ” those of protein. Equation (1) indicates that a large aspect ratio could compensate the lack of stiffness of protein because, apart from the mineral volume concentration, it is the combination $G_P \rho^2$ which affects the composite behaviour. The result given by equation (1) reflects the fact that proteins transfer load between mineral platelets via shear, and a large aspect ratio ρ allows the protein to transfer large shear forces via relatively small shear stress.

The fact that the mineral platelets in biomaterials exhibit very large aspect ratios raises the issue of mechanical stability of platelets under compressive loading. During the 18th century, Swiss mathematician Léonard Euler investigated the mechanical properties of slender structures and found that an elastic rod under compression becomes unstable at a critical load (figure 2a). For a rod with a rectangular cross-section, buckling occurs at a critical stress given by

$$\sigma_{cr} = \frac{\pi^2 E}{12\rho^2} \tag{2}$$

where E is the Young’s modulus and ρ is the aspect ratio defined as the length divided by the thickness of the rod. A compressed rod remains straight up to the critical stress; beyond this stress the rod becomes unstable with respect to a lateral perturbation and tends to buckle into a curved profile which may subsequently lead to severe plastic deformation or fracture. The more slender the bar is (the larger the aspect ratio ρ), the lower the buckling stress. The mineral platelets in biological materials have very large aspect ratios (as large as 30–40 in bone) and are embedded in very soft protein matrix. These features can appear to make these platelets vulnerable to buckling. How does nature deal with this challenge?

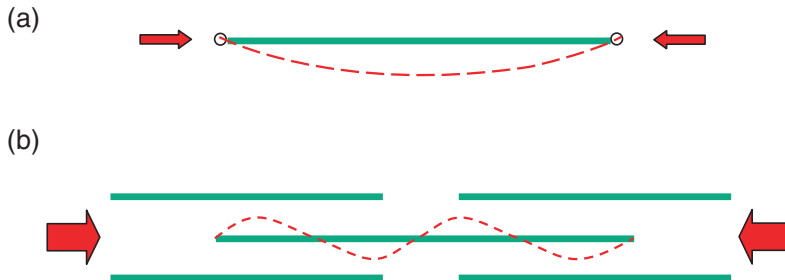


Figure 2. (a) Classical Euler buckling mode of a rod. (b) Schematic illustration of the buckling mode of mineral crystals in biocomposite nanostructures subject to the support of protein within the structure confinement.

§ 2. STABILITY OF MINERAL PLATELETS UNDER COMPRESSION

In the classical Euler buckling, the critical load of a free standing rod corresponds to the lowest buckling mode as shown in figure 2*a*. The mineral crystals in biological materials are expected to have a distinct buckling mode due to the confinement of the surrounding protein–mineral nanostructure. Rosen (1964) studied the buckling of parallel fibres in an elastic matrix and found that their buckling modes can be categorized as shear (in phase) and tension (out of phase) according to the manner of coordination between neighbouring fibres. The staggered alignment (Hodge and Petruska 1963, Jäger and Fratzl 2000) of biomineral crystals is expected to have important influence on their buckling behaviour. So far, it is not clear how staggered mineral platelets would buckle in the biocomposites. As a first step towards an understanding of this issue, we study in this paper the stability of a single mineral platelet confined in an otherwise perfect protein–mineral nanostructure. In this first analysis, we will neglect coordinated buckling between neighbouring mineral platelets.

Figures 1*c* and 1*d* illustrate a compressive stress being imposed on the biological nanostructure. Due to large differences in elastic modulus, mineral platelets bear most of the compressive load and protein transfers force between adjacent mineral platelets via shear (Gao *et al.* 2003, Jäger and Fratzl 2000). As a reasonable approximation, the compressive force on a mineral platelet can be modelled as a uniformly distributed shear stress along the side surfaces of the platelet (figure 1*e*). During buckling, lateral deflections of the mineral platelet will induce a resistance from the surrounding protein. The question is whether the surrounding protein, which has an elastic modulus three orders of magnitude lower than that of mineral, can provide sufficient support to ensure stability of mineral.

Consider a mineral crystal as a rectangular platelet with simply supported ends. With a coordinate system indicated in figure 1*e*, we assume a small lateral deflection in the form of a Fourier series

$$z = \sum_{m=1}^{\infty} \sum_{n=1}^{\infty} a_{mn} \sin \frac{m\pi x}{l} \sin \frac{n\pi y}{w}, \quad (3)$$

where l is the length and w the width of the mineral platelet. We assume that the strain energy stored in the mineral platelet due to compression and the strain energy stored in the protein layer due to shear remain unchanged by the lateral deformation described in equation (3). With this assumption, the change in strain energy in the mineral platelet will be dominated by bending of the platelet and that in the protein layer will be dominated by tension/compression across the layer width. According to Timoshenko and Gere (Timoshenko and Gere 1961), the bending energy of an elastic platelet under deformation profile of equation (3) is

$$\Delta U = \frac{lw}{8} D \sum_{m=1}^{\infty} \sum_{n=1}^{\infty} a_{mn}^2 \left(\frac{m^2 \pi^2}{l^2} + \frac{n^2 \pi^2}{w^2} \right)^2, \quad (4)$$

where

$$D = \frac{E_M h_M^3}{12(1 - \nu^2)} \quad (5)$$

is the bending rigidity, E_M is the Young's modulus, ν the Poisson ratio and h_M the thickness of the mineral platelet; $h_M \ll l, w$. Neglecting coordinated buckling between neighbouring platelets, the change in strain energy stored in the protein layer adjacent to the mineral platelet induced by the deformation of mineral is

$$\Delta V = \frac{1}{2} \int_0^w \int_0^l (2E_p) \left(\frac{z}{h_p}\right)^2 h_p dx dy = \frac{E_p l w}{4h_p} \sum_{m=1}^{\infty} \sum_{n=1}^{\infty} a_{mn}^2, \tag{6}$$

where E_p is the Young's modulus and h_p the thickness of the protein layer between two adjacent mineral platelets. A similar expression has been assumed for the tension mode of coordinated buckling of parallel fibres by Rosen (1964). The work done by the shear force τ due to the deflection of mineral platelet is obtained as,

$$\Delta T = \int_0^w \int_0^{l/2} (2\tau) dx \int_x^{l/2} \frac{1}{2} \left(\frac{\partial z}{\partial \hat{x}}\right)^2 d\hat{x} dy + \int_0^w \int_{l/2}^l (2\tau) dx \int_{l/2}^x \frac{1}{2} \left(\frac{\partial z}{\partial \hat{x}}\right)^2 d\hat{x} dy, \tag{7}$$

which can be simplified via integration by parts as

$$\Delta T = \int_0^w \int_0^{l/2} \tau x \left(\frac{\partial z}{\partial x}\right)^2 dx dy + \int_0^w \int_{l/2}^l \tau (l-x) \left(\frac{\partial z}{\partial x}\right)^2 dx dy. \tag{8}$$

Note the change of direction of the shear stress τ from region $(0, l/2)$ to $(l/2, l)$. Integration of equation (8) yields

$$\Delta T = \frac{w\tau}{16} \sum_{m=1}^{\infty} \sum_{n=1}^{\infty} a_{mn}^2 (m^2 \pi^2 - 2 + 2(-1)^m) + \frac{w\tau}{2} \sum_{m=1}^{\infty} \sum_{n=1}^{\infty} \sum_{k=1, k \neq m}^{\infty} a_{mn} a_{kn} p(m, n, k), \tag{9}$$

where

$$p(m, n, k) = km \left(k^2 + m^2 - 2(k^2 + m^2) \cos\left(\frac{k\pi}{2}\right) \cos\left(\frac{m\pi}{2}\right) + (k^2 + m^2) \cos k\pi \cos m\pi - 4km \sin\left(\frac{k\pi}{2}\right) \sin\left(\frac{m\pi}{2}\right) \right) / ((k-m)^2 (k+m)^2) \tag{10}$$

The critical value of τ associated with the buckling mode (m, n) can be obtained by energy balance,

$$\Delta T = \Delta U + \Delta V, \tag{11}$$

which leads to the following relation in terms of the critical shear stress on mineral

$$\tau_{cr} = \frac{\frac{\pi^4 l D}{8} \sum_{m=1}^{\infty} \sum_{n=1}^{\infty} a_{mn}^2 \left(\frac{m^2}{l^2} + \frac{n^2}{w^2}\right)^2 + \frac{E_p l}{4h_p} \sum_{m=1}^{\infty} \sum_{n=1}^{\infty} a_{mn}^2}{\sum_{m=1}^{\infty} \sum_{n=1}^{\infty} a_{mn}^2 \left(\frac{m^2 \pi^2}{16} + \frac{-2+2(-1)^m}{16}\right) + \frac{1}{2} \sum_{m=1}^{\infty} \sum_{n=1}^{\infty} \sum_{k=1, k \neq m}^{\infty} a_{mn} a_{kn} p(m, n, k)}. \tag{12}$$

Minimizing equation (12) with respect to all coefficients a_{mn} and a_{kn} produces the critical shear stress for buckling. The minimization procedure was discussed by Timoshenko and Gere (1961) who showed that it is often reasonable to adopt only one term in the buckling profile as a first order approximation,

$$z = a_{mn} \sin \frac{m\pi x}{l} \sin \frac{n\pi y}{w}. \quad (13)$$

In this case, the solution is reduced to

$$\tau_{cr} = \frac{2\pi^4 l D}{(m^2\pi^2 - 2 + 2(-1)^m)} \left(\frac{m^2}{l^2} + \frac{n^2}{w^2} \right)^2 + \frac{4E_p l}{(m^2\pi^2 - 2 + 2(-1)^m)h_p}. \quad (14)$$

The second term in equation (14) is due to the effect of protein. The solution in equation (14) indicates that the critical load depends not only on the bending rigidity and the length of mineral platelets, but also on the elastic property as well as the dimensions of the protein matrix.

It is clear from equation (14) that the minimum critical stress is reached when n is equal to 1. If we further assume $l=w$ (a square platelet) and substitute equation (5) for D , equation (14) can be further reduced to

$$\tau_{cr} = E_p \left[\frac{\pi^4(m^2 + 1)^2}{6(m^2\pi^2 - 2 + 2(-1)^m)} \frac{E_M}{E_p \rho^3(1 - \nu^2)} + \frac{4}{m^2\pi^2 - 2 + 2(-1)^m} \frac{\rho \Phi_M}{1 - \Phi_M} \right], \quad (15)$$

where $\Phi_M = h_M/(h_M + h_p)$ is the mineral volume fraction and $\rho = l/h_M$ is the aspect ratio of the mineral platelets.

According to Gao *et al.* (2004) and Ji and Gao (2004b), the compressive stress, σ , imposed on the composite nanostructure is related to the shear stress τ along the mineral platelet by

$$\sigma = \frac{1}{2} \rho \Phi_M \tau. \quad (16)$$

From equations (15) and (16), the critical buckling stress of the embedded mineral platelet associated with a given buckling mode m is

$$\sigma_{cr} = E_p \left[\frac{\pi^4(m^2 + 1)^2}{12(m^2\pi^2 - 2 + 2(-1)^m)} \frac{E_M \Phi_M}{E_p \rho^2(1 - \nu^2)} + \frac{2}{m^2\pi^2 - 2 + 2(-1)^m} \frac{\rho^2 \Phi_M^2}{1 - \Phi_M} \right]. \quad (17)$$

Minimizing equation (17) with respect to all m yields the lowest buckling stress, $\hat{\sigma}_{cr}$.

The buckling behaviour of the biomineral platelets with protein support, as described by equation (17), is drastically different from a free standing platelet. The lowest buckling stress now occurs in a much higher buckling mode with a large wave number m due to protein support and the nanostructure confinement, as illustrated by figure 2b. The buckling mode giving rise to the lowest buckling stress can be called the most favoured mode. Figure 3 shows the most favoured wave number m as a function of the aspect ratio of mineral for two values of mineral volume fraction. It is seen that the most favoured mode m increases with the mineral aspect ratio. For large aspect ratios, the relevant buckling mode $m \gg 1$, in which case the terms of $-2 + 2(-1)^m$ can be neglected so that equation (17) can be further simplified to

$$\sigma_{cr} = E_p \left[\frac{\pi^2 m^2}{12} \frac{E_M \Phi_M}{E_p \rho^2(1 - \nu^2)} + \frac{2}{m^2\pi^2} \frac{\rho^2 \Phi_M^2}{1 - \Phi_M} \right]. \quad (18)$$

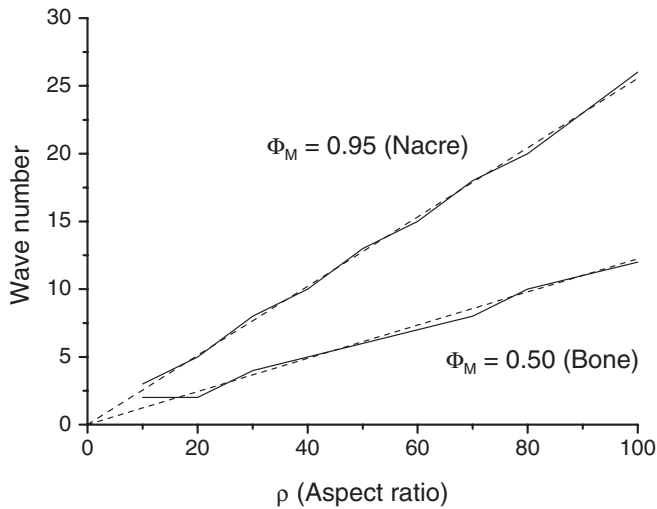


Figure 3. The wave number of the most favoured buckling mode versus the aspect ratio of mineral crystals at two different values of mineral volume concentration. The dashed lines are the prediction of equation (19); the solid lines are predictions by minimizing equation (17).

Minimizing equation (18) with respect to m yields the most favoured buckling mode,

$$\hat{m} \approx \left(\frac{24\Phi_M E_P (1 - \nu^2)}{\pi^4 E_M (1 - \Phi_M)} \right)^{1/4} \rho. \tag{19}$$

Equation (19) demonstrates that, in the limiting case of $m \gg 1$, the most favoured buckling mode increases proportionally with the aspect ratio of mineral. This is in contrast to the classical Euler buckling solution in which the most favoured buckling mode is independent of the aspect ratio of the structure. The approximately linear relationship of equation (19) can also be seen from the more precise solution in figure 3. The volume concentration of mineral can also influence buckling of mineral, as illustrated in figure 3. Alternatively, one can obtain the wavelength of the most favoured buckling mode from equation (19) as,

$$\lambda = \frac{l}{m} \approx \left(\frac{\pi^4 E_M \Phi_M^3}{24 E_P (1 - \nu^2) (1 - \Phi_M)^3} \right)^{1/4} h_P. \tag{20}$$

Equation (20) indicates that the most favoured buckling wavelength is proportional to the thickness of protein channel between adjacent mineral platelets. Apparently, the elastic support and the confinement of adjacent minerals can play a critical role in determining the most favoured buckling mode of the embedded mineral platelets.

It is interesting to note that, in the absence of protein support, the critical stress at buckling becomes

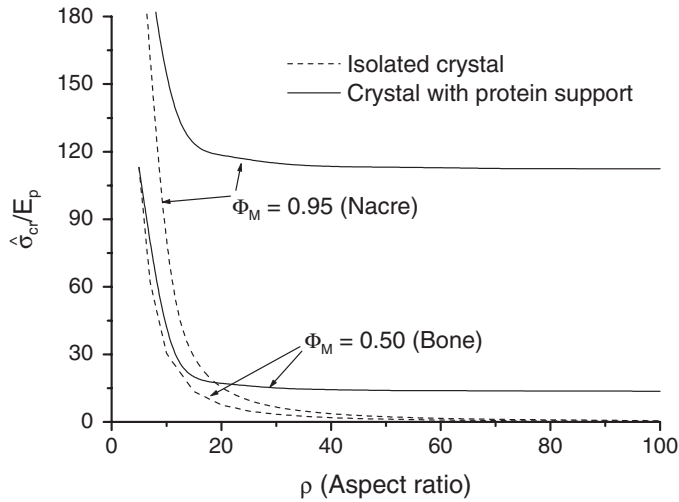


Figure 4. The buckling stress of biological nanostructure versus the aspect ratio of the mineral crystals. The solid curves are for mineral crystals in the biological nanostructure at two different values of mineral volume concentration. Each curve is approaching an asymptotic value (low threshold) predicted by equation (23). The corresponding value of a free standing mineral crystal is plotted for comparison.

$$\sigma_{cr}^* = \frac{\pi^4(m^2 + 1)^2 \Phi_M}{12(m^2 \pi^2 - 2 + 2(-1)^m)(1 - \nu^2)} \frac{E_M}{\rho^2}, \quad (21)$$

where the lowest critical stress occurs when $m=2$ (The buckling associated with mode $m=2$ is slightly lower than that associated with $m=1$),

$$\hat{\sigma}_{cr}^* = \frac{25\pi^2 \Phi_M}{48(1 - \nu^2)} \frac{E_M}{\rho^2}. \quad (22)$$

In this case, the critical stress is inversely proportional to the square of the aspect ratio of mineral platelets, similar to the classical Euler solution of equation (2).

Figure 4 plots the normalized critical stress $\hat{\sigma}_{cr}/E_p$ as a function of the aspect ratio of mineral at two different values of mineral volume concentration. The corresponding curves for $\hat{\sigma}_{cr}^*/E_p$ in the absence of protein support are also plotted for comparison. It is seen that protein can effectively stabilize mineral crystals against buckling, especially at high mineral volume concentration. The stabilizing effect of the protein becomes more profound for larger aspect ratios and higher volume concentrations of the mineral phase. For example, in nacre ($\Phi_M=95\%$, $\rho \sim 10$), the presence of protein increases the critical stress for buckling by 2.5 times in comparison with the isolated crystal; in bones ($\Phi_M=50\%$, $\rho \sim 40$), the critical stress increases by 7.5 times, as indicated in figure 4. At a given volume concentration of protein, the critical stress approaches a constant limited value as the aspect ratio increases, which can be derived by substituting equation (19) into equation (18),

$$\hat{\sigma}_{cr}|_{m \gg 1} = \sqrt{\frac{2E_M E_P \Phi_M^3}{3(1-\nu^2)(1-\Phi_M)}}. \quad (23)$$

In contrast to Euler buckling where the critical load decreases with increasing aspect ratio, equation (23) indicates that the critical buckling stress becomes independent of the aspect ratio of mineral platelets when the aspect ratio is sufficiently large. This provides a lower threshold value below which the mineral platelets will never buckle no matter how large the aspect ratio is or how slender the mineral crystals are. Figure 4 clearly shows this transition (indicated by the arrows). It is interesting to note that the typical aspect ratios of mineral crystals in biological materials, such as bone and shell are large enough and just fall in the transition region.

A result somewhat similar to equation (23) was obtained by Rosen (1964) for the tension mode of coordinated buckling of parallel fibres. Rosen noted that the coordination between neighbouring parallel fibres may involve another mode of coordinated buckling, called the shear mode in which the deformation of a fibre is out-of-phase with its neighbours. According to Rosen's analysis, the tension mode tends to dominate at low and high (above 90%) volume concentrations of the fibre, and the shear mode dominates at intermediate volume concentrations. We expect that the large modulus ratio between the mineral inclusions and the protein matrix as well as the staggered alignment of mineral crystals should significantly influence the coordinated buckling behaviour of biocomposites. A systematic study of coordinated buckling of staggered platelets is beyond the scope of this paper and will be pursued in the near future.

§ 3. SUMMARY

The stability of a single mineral platelet confined in an otherwise perfect protein–mineral nanostructure under compressive loading has been investigated in this paper. This study complements our previous studies on the fracture strength and other mechanical properties of biological materials (Gao *et al.* 2003, 2004, Ji and Gao 2004a,b). Our analysis shows that protein, despite its very low elastic modulus in comparison with mineral, can play an important role in stabilizing mineral particles against buckling. Due to the elastic support of protein and the confinement of the staggered adjacent mineral platelets, the critical buckling mode of the platelet is shifted to a much higher wave number. In the classical Euler buckling, the critical buckling mode is independent of the aspect ratio of the structure and the buckling stress scales with the inverse square of the aspect ratio. In contrast, the critical buckling wave number for the composite nanostructure of biological materials is found to be proportional to the aspect ratio of the mineral, and the critical stress for buckling is found to have a lower threshold value independent of the aspect ratio. These findings are summarized in equation (20) for the critical buckling mode and in equation (23) for the critical buckling stress. In particular, equation (23) shows that the buckling stress in composite nanostructure is proportional to the geometric means of Young's moduli of protein and mineral, and can be amplified by increasing the volume concentration of mineral. It is therefore not surprising that the mineral volume concentration is as high as 95% in sea shells such as nacre whose primary structural functions are to resist compressive loading due to external pressure.

In biological materials, small variations in geometrical parameters such as crystal size and shape are inevitable. From the robustness point of view, the composite

behaviour of materials should not depend sensitively on small variations in structure geometry. We have previously shown (Gao *et al.* 2003) that the nanoscale size of mineral crystals allows them to retain their theoretical tensile strength independent of the structure size and without sensitivity to the potential flaws in the structure. The existence of a constant buckling strength of the composite nanostructure independent of the mineral aspect ratio can further ensure that the nanostructure is robust under compressive loading. The typical aspect ratio of mineral crystals in bone and nacre are large enough to ensure a constant buckling strength for the composite nanostructure. Therefore, it seems that robust design is a key feature in natural evolution of biological materials and this principle should provide guidance for the development of biomimicking nanomaterials (Tang *et al.* 2003).

Finally, we caution that in this first analysis of buckling of biological nanostructure, we have focused on the stability of a single mineral platelet confined in an otherwise perfect protein–mineral nanostructure. While this analysis provides some physical insights on the effect of protein in stabilizing slender mineral particles in biological materials, it may be overly simplistic in many aspects and may not be able to provide an accurate prediction of the compressive strength of biocomposites. It will be critically important in the future to conduct a systematic investigation of the coordinated buckling behaviour in protein–mineral nanostructures.

ACKNOWLEDGEMENTS

This work is supported by the Max Planck Society of Germany, the Overseas Young Investigator Award by the National Science Foundation of China and the Chang Jiang Scholar programme by the Ministry of Education of China. KJH is supported by NSF Grant No. CMS 98-72306. We acknowledge a helpful discussion with Dr. Bin Liu of Max Planck Institute for Metals Research.

REFERENCES

- CURREY, J. D., 1977, *Proc. R. Soc. London B*, **196**, 443.
- FRATZL, P., JAKOB, H. F., RINNERHALER, S., ROSCHGER, P., and KLAUSHOFER, K., 1997, *J. appl. Crystallogr.*, **30**, 765.
- GAO, H., and JI, B., 2003, *Engng. Fract. Mech.*, **70**, 1777.
- GAO, H., JI, B., BUEHLER, M. J., and YAO, H., 2004, *Mech. Chem. Biosystems*, **1**, 37.
- GAO, H., JI, B., JÄGER, I. L., ARTZ, E., and FRATZL, P., 2003, *Proc. Natn. Acad. Sci. U.S.A.*, **100**, 5597.
- HODGE, A. J., and PETRUSKA, J. A., 1963, *Aspects of Protein Structure*, edited by G. N. Ramachandran (New York: Academic Press).
- JÄGER, I., and FRATZL, P., 2000, *Biophys. J.*, **79**, 1737.
- JACKSON, A. P., VINCENT, J. F. V., and TURNER, R. M., 1988, *Proc. R. Soc. London B*, **234**, 415.
- Ji, B., and GAO, H., 2004a, *Mater. Sci. Engng. A*, **366**, 96.
- Ji, B., and GAO, H., 2004b, *J. Mech. Phys. Solids*, **52**, 1963.
- KAMAT, S., SU, X., BALLARINI, R., and HEUER, A. H., 2000, *Nature*, **405**, 1036.
- LANDIS, W. J., 1995, *Bone*, **16**, 533.
- LANDIS, W. J., and HODGENS, K. J., 1996, *J. Struct. Boil.*, **117**, 24.
- MENIG, R., MEYERS, M. H., MEYERS, M. A., and VECCHIO, K. S., 2000, *Acta mater.*, **48**, 2383.
- MENIG, R., MEYERS, M. H., MEYERS, M. A., and VECCHIO, K. S., 2001, *Mater. Sci. Engng. A*, **297**, 203.
- RHO, J. Y., KUHN-SPEARING, L., and ZIOUPOS, P., 1998, *Med. Engng. Phys.*, **20**, 92.
- ROSEN, B. W., 1964, Paper presented at the American Society for Metals Seminar on Fibre Composite Materials, Metals Park, OH, 17–18 October.

- TANG, Z., KOTOV, N., MAGONOV, S., and OZTURK, B., 2003, *Nature mater.*, **2**, 413.
- TESCH, W., EIDELMAN, N., ROSCHGER, P., GOLDENBERG, F., KLAUSHOFER, K., and FRATZL, P., 2001, *Calcif. Tissue Int.*, **69**, 147.
- TIMOSHENKO, S. P., and GERE, J. M., 1961, *Theory of Elastic Stability* (New York: McGraw-Hill).
- WANG, R. Z., SUO, Z., EVANS, A. G., YAO, N., and AKSAY, I. A., 2001, *J. Mater. Res.*, **16**, 2485.
- WEINER, S., and WAGNER, H. D., 1998, *Ann. Rev. Mater. Sci.*, **28**, 271.